PHYSICAL REVIEW B **89**, 180402(R) (2014)

Magnetic structure in epitaxially strained Sr_2CrReO_6 thin films by element-specific XAS and XMCD

Adam J. Hauser,[1] Jeremy M. Lucy,[2] Michael W. Gaultois,[3] Molly R. Ball,[4] Jennifer R. Soliz,[5] Yongseong Choi,[6] Oscar D. Restrepo,[4] Wolfgang Windl,[4] John W. Freeland,[6] Daniel Haskel,[6] Patrick M. Woodward,[5] and Fengyuan Yang[2]

[1]*California Nanosystems Institute, University of California, Santa Barbara, California 93106, USA*

[2]*Department of Physics, The Ohio State University, Columbus, Ohio 43210, USA*

[3]*Materials Research Laboratory, University of California, Santa Barbara, California 93106, USA*

[4]*Department of Materials Science and Engineering, The Ohio State University, Columbus, Ohio 43210, USA*

[5]*Department of Chemistry, The Ohio State University, Columbus, Ohio 43210, USA*

[6]*Advanced Photon Source, Argonne National Laboratory, Argonne, Illinois 60439, USA*

(Received 28 December 2013; published 8 May 2014)

We have analyzed the magnetic configuration for highly ordered Sr_2CrReO_6 films as a function of epitaxial strain using magnetometry and x-ray magnetic circular dichroism (XMCD) measurements of Cr, Re, and O sites. The in-plane magnetic moments change significantly when tensile strain is applied. O K-edge XMCD indicates that O sites carry at least a portion of the bulk magnetization. Spin moment values measured for Cr match calculations incorporating spin-orbit effects, while both spin and orbital moments measured for Re sites are slightly higher than previously predicted. Finally, we discuss large changes in the x-ray absorption near-edge structure that are observed at the Cr and Re L edges due to epitaxial strain.

DOI: 10.1103/PhysRevB.89.180402 PACS number(s): 75.50.Pp, 75.50.Gg, 75.70.Tj, 78.20.Ls

Sr_2CrReO_6 (SCRO) has proven to be a highly interesting double perovskite material due to the convergence of many attractive properties: a Curie temperature well above 300 K [1–4] enabling room temperature applications, a scientifically interesting double exchange phenomenon that suggests high spin polarization for spintronic applications [5–7], significant spin-orbit interactions and correlated electron behavior due to the presence of Re 5d orbitals, and the recently discovered semiconducting behavior in highly ordered epitaxial films which, combined with high temperature ferrimagnetism, may be useful in nonvolatile logic devices [3,8]. Progress toward device applications, however, will require an in-depth understanding of the electronic and magnetic configurations of the system.

Theoretical modeling has suggested a double perovskite double exchange model, wherein the Cr 3d and Re 5d orbitals are hybridized via the oxygen 2p orbitals [5,6,9,10]. In these models, the rocksalt ordered Cr and Re atoms have oppositely aligned spin moments and almost exclusively account for the magnetization in the system. Previously, element-specific x-ray magnetic circular dichroism (XMCD) measurements of the Re site in polycrystalline bulk samples have been studied [11], but to date such work on highly ordered crystalline materials has not been undertaken, and no measurements to characterize the Cr or O sites in bulk or thin film have been reported. The L-edge x-ray absorption near-edge structure (XANES) of Cr and Re can be analyzed to provide significant information regarding orbital configuration and bonding environments. By applying varying epitaxial strain to Sr_2CrReO_6 thin films, we can draw conclusions from the system's reaction to the induced distortions. These results are needed to properly test our understanding of this material system.

Epitaxial SCRO films were grown by off-axis magnetron sputtering as previously described and characterized [3] on $(LaAlO_3)_{0.3}(Sr_2AlTaO_6)_{0.7}$ (LSAT) and $SrTiO_3$ (STO) substrates, as well as on LSAT substrate with a fully relaxed Sr_2CrNbO_6 (SCNO) buffer layer. These substrates impart 0.78% compressive (LSAT), 0.17% tensile/nominally relaxed (STO), and 1.09% tensile (SCNO/LSAT) strains upon their respective SCRO films. All films were grown to a thickness of 90 nm, as confirmed by modeling of Laue oscillations seen in x-ray diffraction spectra. A Quantum Design superconducting quantum interference device (SQUID) magnetometer was used to characterize the in-plane magnetization.

Element-specific x-ray absorption spectroscopy (XAS) and XMCD measurements of the Cr L, O K, and Re L edges were then taken at the soft (Cr, O, 4-ID-C) and hard (Re, 4-ID-D) x-ray beam lines at the Advanced Photon Source, Argonne National Laboratory. The soft x-ray measurements were taken in the surface sensitive total electron yield mode, with the applied magnetic field offset 10° from the plane of the film surface. The hard x-ray measurements were taken in glancing angle fluorescence mode to optimize probed volume at the higher energy of Re L edges, with the plane of the film tilted 3.8(1)° with respect to the applied magnetic field. Edge energies were calibrated with standards at known energies (e.g., Cr_2O_3 for the Cr L edge, and W foil for the Re L edge). Systematic error introduced by the placement of the absorption edge step is the dominant source of error in our XMCD measurements, so we have analyzed the data for the range of all reasonable step edge centroid energies, and report the average moment and error values consummate with the range of possible moments calculated. Within the ranges of error we report, the choice of placing the step edge at the white line maximum intensity will generally correspond with the lower magnitude moment values. Placing the step edge at the maximum derivative of the XAS (center of rising edge) with respect to energy will yield magnitude moment values in the upper end of the error range. The hole number values used in this work are the result of theoretical calculations and cannot be assigned a quantitative error bar, and thus add further uncertainty to our results.

In-plane magnetic hysteresis loops for the three SCRO films at temperature $T = 200$ K are shown in Fig. 1. Experimental limitations of the 4-ID-D beamline at the time of the experiment imposed a maximum measurement field of 3.5 T,

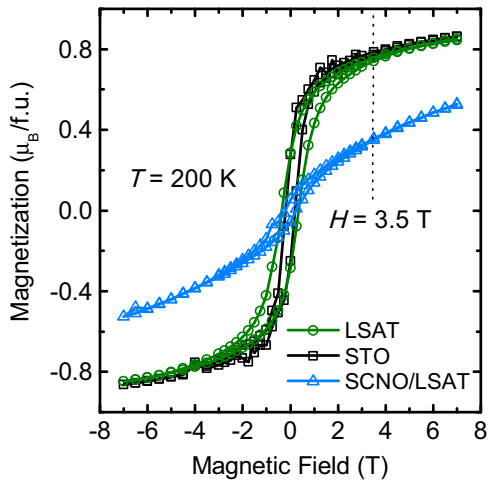

FIG. 1. (Color online) In-plane magnetic hysteresis loop at T = 200 K for films on (001)-oriented LSAT (green circles), $SrTiO_3$ (black squares), and ~200 nm Sr_2CrNbO_6 buffer layer on LSAT (blue triangles).

which suffices to largely saturate each film at 200 K. At 3.5 T (shown in Fig. 1 as a vertical dashed line), the magnetization of films grown on LSAT, STO, and SCNO/LSAT are 0.76 μ_B, 0.79 μ_B, and 0.36 μ_B per formula unit (f.u.), respectively. These numbers represent the "macroscopic" total moment of the SCRO unit cell and will be compared to the individual Cr and Re moments. It should be noted that the film under large tensile strain (SCRO/SCNO/LSAT) has a relatively small in-plane moment compared to compressive (SCRO/LSAT) or small tensile (SCRO/STO) strains. Such a significant drop in moment is not due to loss of crystallinity or decreased Cr/Re cation order as indicated by our previous work [3,12,13], which shows evidence of high crystallinity in all strained films by x-ray diffraction.

Figure 2 shows a full summary of the Cr L-edge, Re L-edge, and O K-edge XANES and XMCD spectra for all three films. All L-edge data is normalized to a 2:1 L_3/L_2 edge jump ratio. Spin (m_S) and orbital (m_L) moments were then extracted by sum rule analysis [14,15]. Due to the narrow $2p$ spin-orbit splitting in Cr and the resultant quantum mechanical mixing of $j_{1/2}$ and $j_{3/2}$ excitations, a spin correction factor of 2 was applied for all three Cr spectra [16]. To analyze these data, we use density functional theory (DFT) to calculate the number of holes for each system. We use projector augmented-wave pseudopotentials [17] as implemented in the Vienna *ab initio* simulation package (VASP) [18,19]. Correlation effects were treated within the generalized gradient approximation+U approach [20] with a value of U = 3 eV and an exchange parameter J = 0.87 eV for the Cr d orbitals [21]. We have relaxed the atomic positions within the Sr_2CrReO_6 unit cells for the different strains using the experimental lattice parameters. The number of valence electrons occupying an orbital can be obtained by integrating its partial density of states up to the Fermi level, which subtracted from 10, gives the number of holes. We obtain 5.69 (5.17), 5.72 (5.28), and 5.68 (5.28) holes for Cr (Re) in SCRO/LSAT, SCRO/SCNO/LSAT, and SCRO/STO, which lead to the calculated averaged spin moments of 1.48 (− 0.68), 1.50 (− 0.69), and 1.49 (− 0.68), respectively. The measured spin and orbital moments for the Cr and Re sites are shown in their respective spectra.

We again note the stark difference in the results of the SCRO films on LSAT and STO as compared to the film on SCNO/LSAT. On the Re site, both the spin and orbital moments are reduced by roughly a factor of 3, and the Cr spin moment sharply decreases in magnitude. Given this information and the shape of the hysteresis loop, it is likely that a strong anisotropy turns the magnetic easy axis out of plane and, consequently, an in-plane field of 3.5 T cannot align the SCRO magnetization. Determination of magnetocrystalline anisotropy requires careful comparison of the in-plane and out-of-plane magnetizations, coercive fields, and anisotropy fields, and is the subject of a more detailed study [22].

Figures 2(a) and 2(b) show the Cr XMCD spectra for films grown on LSAT and STO, respectively, which indicate strongly quenched orbital moments and spin moments antiparallel to that of Re, as expected in ferrimagnetic SCRO. The respective spin moments of 1.10(1) μ_B/f.u. (LSAT) and 1.26(1) μ_B/f.u. (STO) for Cr are smaller than our calculated values (1.48 and 1.49 μ_B/f.u., respectively). However, it is important to note that the calculated values represent a material system at T = 0 K and full magnetic saturation. It is clear from Fig. 1 that at T = 200 K, an applied field of 3.5 T does not fully saturate any film in this study. From previous work, we can conservatively expect a 10%–15% loss as compared to the calculated magnetization due to thermal energy, and another 10%−15% loss due to incomplete magnetization [3]. This already accounts for the difference between experiment and theory, even without considering the small decrease in magnetization expected from Cr/Re antisite disorder.

Figures 2(d) and 2(e) show the Re XMCD spectra for films grown on LSAT and STO, which yield m_S and m_L values matching closely with previous theoretical predictions [10,23] as well as our calculations and bulk powder XMCD results [11]. The opposite signs of the spin and orbital moments are as expected for a less than half-filled shell with spin-orbit coupling. However, by applying the same considerations in the Cr spectra with incomplete magnetic saturation at finite measurement temperature, the projected "fully saturated" spin and orbital moment values may be slightly higher than previously predicted.

When the combined spin and orbital moments for Cr and Re are added together, the XMCD spectra imply total moments of 0.62(6) and 0.71(5) μ_B/f.u. for films on LSAT and STO, respectively. Comparing these values to the macroscopic magnetizations found by SQUID magnetometry, we find that 0.14(6) μ_B/f.u. (LSAT) and 0.08(5) μ_B/f.u. (STO) are unaccounted for in the "B-site only" model.

There are two primary sources for the missing moment. It could either simply reside on the O $2p$ orbitals, and/or the neglect of a magnetic dipole moment T_z in the spin sum rule for Re could contribute to the unaccounted moment [15]. The latter is possible since sizable spin-orbit interactions are known to occur in $5d$ elements such as Re [24], and can contribute to T_z to some degree. Deviations in the octahedral environment may also contribute to T_z. Although strain is well known to produce effects such as octahedral rotations, tilting, and Jahn-Teller distortions [25,26], we see a similar discrepancy for strained and unstrained films alike.

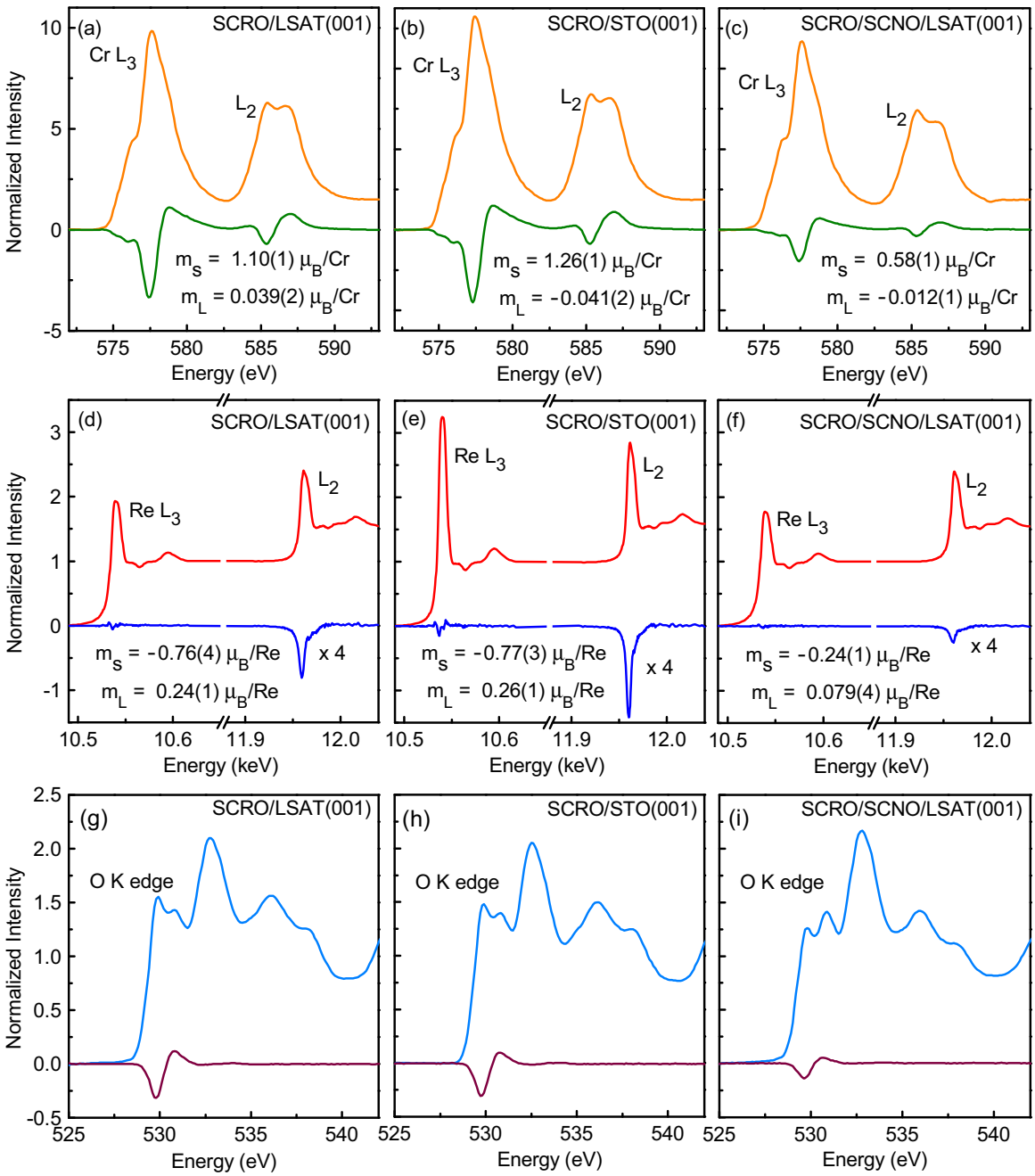

FIG. 2. (Color online) Normalized XANES and XMCD spectra at the (a)–(c) Cr L, (d)–(f) Re L, and (g)–(i) O K edges. XANES (XMCD) spectra are on top (bottom) within each figure. Spin and orbital moments are given for the Cr and Re spectra.

Between these two, our data indicate that magnetic moments on the O $2p$ orbitals should be the dominant contribution, since we have found evidence of magnetic moment in the oxygen $2p$ orbitals by measuring the O K-edge spectra, as shown in Figs. 2(g)–2(i) for all three films. Quantitatively, our DFT calculations yield a total moment of 0.02 μ_B/oxygen for all three epitaxial strains, which matches well with the equivalent missing moment (~0.01–0.03 μ_B/oxygen) in our experiment. The existence of moments on the oxygen sites can be understood by the fact that when the double exchange model is applied to double perovskite systems, there is a high degree of orbital hybridization of B-site cations (in this case, Cr and Re) mediated by each intervening oxygen [6]. Our findings are also consistent with previous work that found that CrO_2 had significant spin moments on the oxygen site due to Cr $3d$-O $2p$ hybridization [10,27,28]. It is not uncommon for double perovskites to have oxygen with magnetic moments above this range. For instance, our results are in line with previous work that found that Sr_2FeMoO_6 has a magnetic moment on oxygen between 0.06 μ_B/oxygen and 0.09 μ_B/oxygen [29].

Figures 3(a) and 3(b) show the overlaid Cr L and Re L_2 x-ray absorption spectra for all three films, which result from excitation of $2p$ electrons to unoccupied d states. The line shapes are sensitive to changes in coordination geometry, and the edge absorption energy given by the inflection point is sensitive to changes in bonding and charge density [30,31].

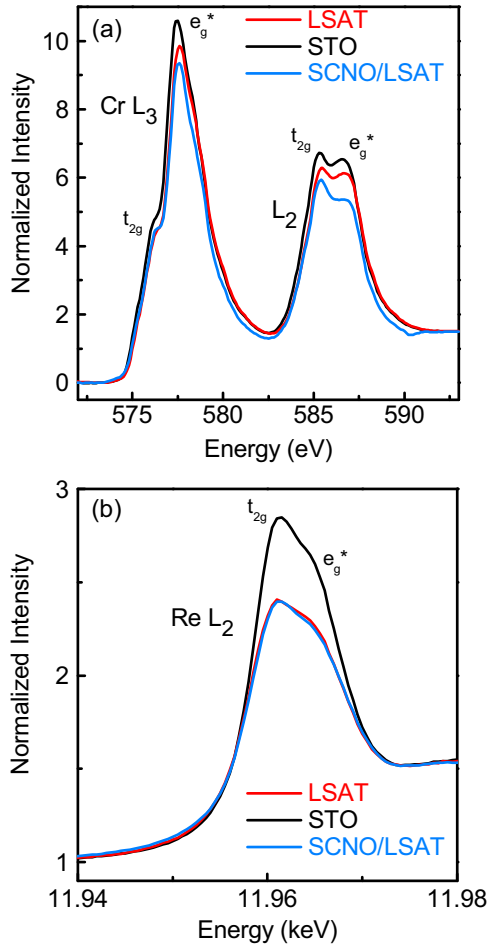

FIG. 3. (Color online) Normalized x-ray absorption spectra for different strains at the (a) Cr $L_{2,3}$ edges and (b) Re L_2 edge.

Figure 3(a) shows the Cr L_3 edge, where the absorption energy increases by 0.25 eV under both ∼1% compressive and tensile strain when compared to the nominally unstrained Sr_2CrReO_6 film grown on STO. The absorption peak maximum exhibits an identical shift. The change in the Cr L_3 edge energy is small compared to shifts seen in Cr compounds due to changes in Cr formal charge [32], suggesting epitaxial strain has only a weak influence on the Cr ground state electron density. In general, a decrease in Cr L-edge absorption energy is caused by higher charge density on Cr, which leads to a lower effective nuclear charge. This destabilizes the electronic levels and decreases the energy required to promote core electrons to unoccupied states.

The Cr L edge also undergoes minor changes in spectral line shape with strain, but the line shapes of 3d L-edge spectra are complicated by multiplet effects. These multiplet effects are caused by the overlap of partially filled core and valence wave functions in the final state, which makes interpretation difficult by altering the line shape and intensity ratios of the resulting spectra [33]. (The large 2p spin-orbit coupling in 5d systems reduces the influence of multiplet effects in Re 5d L-edge spectra discussed later, which makes interpretation of Re L-edge spectra more feasible.) The t_{2g}/e_g^* intensity ratio in the Cr L_2 edge is ∼1.03 in epitaxial Sr_2CrReO_6 films on LSAT and STO, but is 1.11 in films on SCNO/LSAT, a 7.7% change. Similarly, the L_3 t_{2g}/e_g^* intensity ratio increases by 5.2% on SCNO/LSAT. Although there is a significant change in the line shape of the films grown under 1.09% tensile strain on SCNO/LSAT, these films are complicated by the presence of the strong magnetic anisotropy discussed earlier. No significant change in line shape is seen in films grown on LSAT under 0.78% compressive strain. The L_3/L_2 integrated area branching ratios are 1.47 and 1.48 for films grown on STO and LSAT, and 1.64 for films grown on SCNO/LSAT. Overall, there are only small changes between films grown on LSAT and those grown on STO, and although there are slightly larger changes in films grown on SCNO/LSAT, drawing conclusions from the Cr L edge is not straightforward given the many aforementioned considerations.

The Re L-edge spectra of Sr_2CrReO_6 films show more significant changes. The Re L_3 edge absorption energy (given by the inflection point) decreases by ∼1 eV under ∼1% applied tensile or compressive strain (0.78% compressive strain: $\Delta E_{(\mathrm{STO-LSAT})} = -1.2$ eV, 1.09% tensile strain: $\Delta E_{(\mathrm{STO-SCNO/LSAT})} = -1.0$ eV). The L_2 edge line shape experiences a corresponding change; the intensity of the primary transition decreases substantially in strained films [shown in Fig. 3(b)], and the L_3 edge white line intensity also decreases by ∼45%. The L_3/L_2 integrated area branching ratios are 1.99 and 2.02 for films grown on STO and LSAT, and 1.62 for films grown on SCNO/LSAT.

In general, the probability of a transition is proportional to the density of unoccupied states, so the intensity of the primary absorption feature (i.e., the L edge white line) is sensitive to changes in the electronic structure. Under most circumstances, the decrease in absorption energy and white line intensity would suggest an increase in the ground state charge density of Re, though the magnitudes of the changes are unexpectedly large given that there is no change in the formal charge of Re. The stability of the Re valence states is supported by DFT calculations performed here, which suggest the number of electrons per Re site increases by 0.1 from films grown on STO to films grown on LSAT. Furthermore, any change in the Re charge would be difficult to reconcile with other sample considerations. Maintaining charge neutrality with considerably more valence electrons in Re would require either oxidation of the Cr—there is no appreciable change in Cr valence states seen by Cr L-edge XANES—or formation of oxygen vacancies commensurate with the change in the Re valence state. However, based on the work by Clancy *et al.*, the change in valence state correlating to the observed absorption energy shift would require nearly two oxygen vacancies per unit cell [34]. Such a large concentration of vacancies would likely have resulted in significant changes to the material properties of the system, but we see no such effects. For instance, oxygen vacancies have been previously reported to lead to rapid relaxation of epitaxial strain in SCRO films [13]. However, off-axis x-ray diffractometry reveals the films in the present work are coherently strained to the substrate, even at film thicknesses of 90 nm.

In the case of SCRO, it is more likely that these changes are the result of the tetragonal distortion of Re centers induced by epitaxial strain. The tetragonal distortion breaks the degeneracy of unoccupied Re states and leads to broadening of

the resulting transitions. In a simple crystal field interpretation, tetragonal distortion splits the partially occupied Re octahedral t_{2g} states, leading to nondegenerate unoccupied states. Instead of a single transition with high intensity in unstrained SCRO, there are several transitions with less intensity in strained samples.

These changes can occur without any change in the Re formal charge. Analogous results have been observed in Al K-edge investigations of regular and distorted Al^{3+} octahedral centers in oxides, where distortion decreases the Al K-edge absorption energy by ∼2 eV and splits the primary absorption feature [35]. In fact, we estimate that the integrated white line intensity shown in that paper decreased by approximately 50% due to octahedral distortion, roughly similar to our observations in SCRO. The same phenomenon is also seen in Ti L-edge spectra of octahedral Ti^{4+} centers in $SrTiO_3$ (regular) and TiO_2 (distorted) [36].

In summary, we have analyzed a strain-dependent series of SCRO films via in-plane SQUID magnetometry and element-specific XANES/XMCD analysis of the Cr and Re $L_{2,3}$ edges. We find a significant change in the in-plane magnetic moment by both techniques when tensile strain is epitaxially applied. For nominally relaxed and compressively strained films, Cr-site XMCD shows a slightly lower spin moment than previously predicted, but matches well with calculations incorporating spin-orbit effects. Re-specific XMCD yields spin and orbital moments that agree well with previous theory and bulk powder results, but considerations of incomplete magnetic saturation suggest calculations may underestimate the ideal spin and orbital moment values. Interestingly, we find a small moment (0.01–0.03 μ_B/oxygen) at the oxygen site, which is confirmed by both theory and experiment. Finally, comparative analysis of Cr and Re L-edge XANES shows that epitaxial strain leads to large changes in the Re ground state, while Cr is largely unaffected.

The authors gratefully acknowledge Richard Rosenberg for assistance in measurements at beamline 4-ID-C, Advanced Photon Source, Argonne National Laboratory. This work is supported by the Center for Emergent Materials at The Ohio State University, a NSF Materials Research Science and Engineering Center (Award No. DMR-0820414). Partial support is provided by the NanoSystems Laboratory at The Ohio State University. Use of the Advanced Photon Source was supported by the US Department of Energy, Office of Science, under Contract No. DE-AC02-06CH11357. A.J.H. acknowledges support through an Elings Prize Fellowship of the California Nanosystems Institute at University of California, Santa Barbara. M.W.G. is supported by a NSERC Postgraduate Scholarship and an International Fulbright Science & Technology Award.

[1] D. Serrate, J. M. De Teresa, and M. R. Ibarra, J. Phys.: Condens. Matter **19**, 023201 (2007).
[2] H. Kato, T. Okuda, Y. Okimoto, Y. Tomioka, Y. Takenoya, A. Ohkubo, M. Kawasaki, and Y. Tokura, Appl. Phys. Lett. **81**, 328 (2002).
[3] A. J. Hauser, J. R. Soliz, M. Dixit, R. E. A. Williams, M. A. Susner, B. Peters, L. M. Mier, T. L. Gustafson, M. D. Sumption, H. L. Fraser, P. M. Woodward, and F. Y. Yang, Phys. Rev. B **85**, 161201 (2012).
[4] H. Asano, N. Kozuka, A. Tsuzuki, and M. Matsui, Appl. Phys. Lett. **85**, 263 (2004).
[5] G. Vaitheeswaran, V. Kanchana, and A. Delin, Appl. Phys. Lett. **86**, 032513 (2005).
[6] O. N. Meetei, O. Erten, A. Mukherjee, M. Randeria, N. Trivedi, and P. Woodward, Phys. Rev. B **87**, 165104 (2013).
[7] S. A. Wolf, D. Awschalom, R. Buhrman, J. Daughton, S. von Molnár, M. Roukes, A. Chtchelkanova, and D. Treger, Science **294**, 1488 (2001).
[8] K. Ando, Science **312**, 1883 (2006).
[9] H. Das, P. Sanyal, T. Saha-Dasgupta, and D. D. Sarma, Phys. Rev. B **83**, 104418 (2011).
[10] G. Vaitheeswaran, V. Kanchana, M. Alouani, and A. Delin, Europhys. Lett. **84**, 47005 (2008).
[11] P. Majewski, S. Geprägs, O. Sanganas, M. Opel, R. Gross, F. Wilhelm, A. Rogalev, and L. Alff, Appl. Phys. Lett. **87**, 202503 (2005).
[12] J. M. Lucy, A. J. Hauser, H. L. Wang, J. R. Soliz, M. Dixit, R. E. A. Williams, A. Holcombe, P. Morris, H. L. Fraser, D. W. McComb, P. M. Woodward, and F. Y. Yang, Appl. Phys. Lett. **103**, 042414 (2013).
[13] A. J. Hauser, J. M. Lucy, H. L. Wang, J. R. Soliz, A. Holcomb, P. Morris, P. M. Woodward, and F. Y. Yang, Appl. Phys. Lett. **102**, 032403 (2013).
[14] B. T. Thole, P. Carra, F. Sette, and G. van der Laan, Phys. Rev. Lett. **68**, 1943 (1992).
[15] C. T. Chen, Y. U. Idzerda, H.-J. Lin, N. V. Smith, G. Meigs, E. Chaban, G. H. Ho, E. Pellegrin, and F. Sette, Phys. Rev. Lett. **75**, 152 (1995).
[16] E. Goering, Philos. Mag. **85**, 2895 (2005).
[17] P. E. Blöchl, Phys. Rev. B **50**, 17953 (1994).
[18] G. Kresse and J. Hafner, Phys. Rev. B **47**, 558(R) (1993).
[19] G. Kresse and J. Hafner, Phys. Rev. B **49**, 14251 (1994).
[20] V. I. Anisimov, J. Zaanen, and Ole. K. Andersen, Phys. Rev. B **44**, 943 (1991).
[21] H.-T. Jeng and G. Y. Guo, Phys. Rev. B **67**, 094438 (2003).
[22] J. M. Lucy (unpublished).
[23] V. Kanchana, G. Vaitheeswaran, and M. Alouani, J. Phys.: Condens. Matter **18**, 5155 (2006).
[24] L. Mattheiss, Phys. Rev. **151**, 450 (1966).
[25] P. M. Woodward, Acta Crystallogr., Sect. B: Struct. Sci. **53**, 32 (1997).
[26] P. M. Woodward, Acta Crystallogr., Sect. B: Struct. Sci. **53**, 44 (1997).
[27] D. J. Huang, H.-T. Jeng, C. F. Chang, G. Y. Guo, J. Chen, W. P. Wu, S. C. Chung, S. G. Shyu, C. C. Wu, H.-J. Lin, and C. T. Chen, Phys. Rev. B **66**, 174440 (2002).
[28] E. Goering, A. Bayer, S. Gold, G. Schütz, M. Rabe, U. Rüdiger, and G. Güntherodt, Europhys. Lett. **58**, 906 (2002).

[29] R. Mishra, O. D. Restrepo, P. M. Woodward, and W. Windl, Chem. Mater. **22**, 6092 (2010).
[30] R. D. Leapman, L. A. Grunes, and P. L. Fejes, Phys. Rev. B **26**, 614 (1982).
[31] J. G. Chen, Surf. Sci. Rep. **30**, 1 (1997).
[32] T. L. Daulton and B. J. Little, Ultramicroscopy **106**, 561 (2006).
[33] F. de Groot, Coord. Chem. Rev. **249**, 31 (2005).
[34] J. P. Clancy, N. Chen, C. Y. Kim, W. F. Chen, K. W. Plumb, B. C. Jeon, T. W. Noh, and Y. J. Kim, Phys. Rev. B **86**, 195131 (2012).
[35] J. A. van Bokhoven, H. Sambe, D. C. Koningsberger, and D. E. Ramaker, J. Phys. IV France **7**, C2-835 (1997).
[36] R. Laskowski and P. Blaha, Phys. Rev. B **82**, 205104 (2010).